

## Accepted Manuscript

The role of UCP 1 in production of reactive oxygen species by mitochondria isolated from brown adipose tissue

Andrea Dlasková, Kieran Clarke, Richard K. Porter

PII: S0005-2728(10)00141-6  
DOI: doi: [10.1016/j.bbabbio.2010.04.008](https://doi.org/10.1016/j.bbabbio.2010.04.008)  
Reference: BBABIO 46493

To appear in: *BBA - Bioenergetics*

Received date: 21 December 2009  
Revised date: 12 April 2010  
Accepted date: 14 April 2010



Please cite this article as: Andrea Dlasková, Kieran Clarke, Richard K. Porter, The role of UCP 1 in production of reactive oxygen species by mitochondria isolated from brown adipose tissue, *BBA - Bioenergetics* (2010), doi: [10.1016/j.bbabbio.2010.04.008](https://doi.org/10.1016/j.bbabbio.2010.04.008)

This is a PDF file of an unedited manuscript that has been accepted for publication. As a service to our customers we are providing this early version of the manuscript. The manuscript will undergo copyediting, typesetting, and review of the resulting proof before it is published in its final form. Please note that during the production process errors may be discovered which could affect the content, and all legal disclaimers that apply to the journal pertain.

The Role of UCP 1 in Production of Reactive Oxygen  
Species by Mitochondria Isolated from Brown Adipose  
Tissue.

Andrea Dlasková, Kieran Clarke and Richard K. Porter

School of Biochemistry and Immunology, Trinity College Dublin, Dublin 2. Ireland.

Key words: mitochondria, reactive oxygen species, brown adipose tissue,  
uncoupling protein 1.

Correspondence: Email: rkporter@tcd.ie, Tel +353-1-896 1617; Fax +353 -1 677 2400

## ABSTRACT

We provide evidence that ablation or inhibition of, uncoupling protein 1 increases the rate of reactive oxygen containing species production by mitochondria from brown adipose tissue, no matter what electron transport chain substrate is used (succinate, glycerol-3-phosphate or pyruvate/malate).

Consistent with these data are our observations that (a) the mitochondrial membrane potential is maximal when uncoupling protein 1 is ablated or inhibited and (b) oxygen consumption rates in mitochondria from uncoupling protein 1 knock-out mice, are significantly lower than those from wild-type mice, but equivalent to those from wild-type mice in the presence of GDP. In summary, we show that uncoupling protein 1 can affect reactive oxygen containing species production by isolated mitochondria from brown adipose tissue.

## 1. Introduction

A byproduct of all normally functioning mitochondria is a continual non-productive release of electrons from the electron transport chain resulting in the production of intracellular reactive oxygen containing species (ROS), such as superoxide. Estimates from in vitro studies have calculated an average of 1-

2% of electrons “escape” from the electron transport chain [1]. Evidence has shown that ROS production rate is greater from mitochondria poised closer to state 4 than those poised closer to state 3, which is consistent with the reduced state of the electron transport chain [2,3] and a driving force for release of ROS being positively correlated with proton electrochemical gradient ( $\Delta p$ ) [4-7]. The sites of ROS production from the electron transport chain are predominantly complex I and III with in vitro evidence showing that oxidation through glycerol-3-phosphate dehydrogenase being a major source of ROS [8-11]. Vulnerable targets of ROS include local sites such as the mitochondrial inner membrane lipids, like cardiolipin [12,13], and polyunsaturated fatty acids in membrane lipids in particular [14]. Oxidation of polyunsaturated fatty acids result in highly reactive aldehydes such as 4-hydroxy-2-nonenals which covalently modify and interfere with protein/enzyme function [15].

However, all cells have antioxidants and antioxidation mechanisms which counteract ROS production by mitochondria to differing extents [6,14,16]. Antioxidant systems associated with mitochondria include ubiquinol [17], glutathione peroxidase [12], vitamin E [18] and manganese dependent superoxide dismutase [19]. A further potential physiological mechanism to alleviate ROS production by mitochondria is termed mild-uncoupling [20]. Mild-uncoupling is based on the observations that uncoupling lowers  $\Delta p$ , decreases the degree of reduction in the electron transport chain and thus will

reduce ROS production from the electron transport chain. Evidence is accumulating to implicate a role for uncoupling proteins in this mild-uncoupling process [21]. The mitochondrial uncoupling proteins, UCP 2 and UCP 3 have been shown to be efficacious in alleviating ROS production in cells/tissue [22,23] and the lack of UCP 2 has been associated with increased ROS production by cells [24,25]. Furthermore, UCP activity has been shown to be activated by fatty acid oxidation products such as 4-hydroxy-2-nonenals [26,27] although the specificity of this observation has been contested [28]. The investigations on the mitochondrial uncoupling protein, UCP 1, have predominantly focused on its key thermogenic role in brown adipose tissue, where it uncouples metabolism from ATP synthesis [29]. In this study we set out, not to determine whether ROS activates UCP 1 but, to determine whether UCP 1 can effect ROS production by brown adipose tissue mitochondria.

## **2. Materials and methods**

### *2.1 Wild Type (WT) and UCP1 knock-out (KO) mice*

Wild Type (C57BL/6J) and UCP1 knock-out (C57BL/6J)[originally from the laboratory of Leslie P. Kozak, Pennington Biomedical Research Center, Baton Rouge, Louisiana, USA] mice were housed in groups of 6 in a specific pathogen free environment. Mice were a mix of males and females aged between 6-10weeks. They were housed at  $25\pm 1^{\circ}\text{C}$  in individually ventilated cages. All animals were allowed free access to food [Harlan 2018 Teklad

Global 18% Protein Rodent diet] and water and a 12-hour light/dark cycle was in place. All mice were killed by CO<sub>2</sub> asphyxiation.

### *2.2 Mitochondria preparation*

BAT mitochondria were prepared by homogenisation followed by differential centrifugation according to the method of Scarpace et al. [30]. Mitochondrial protein concentrations were determined by the bicinchoninic acid method (BCA) [31].

### *2.3 Mitochondrial ROS generation*

H<sub>2</sub>O<sub>2</sub> generation, detected by the Amplex Red II assay, was essentially as described in Dlasková et al. [32]. The assay medium contained mitochondria (0,125 mg/ml), 5µM Amplex Red, 10U/ml of horseradish peroxidase, 30U/ml superoxide dismutase (SOD), 60mM sucrose, 30mM KCl, 20 mM Tris, 1mM ethylenediaminetetraacetic acid (EDTA), 1mM ethylene glycol-bis(β-aminoethyl ether) N,N,N',N'-tetraacetic acid (EGTA), 0.1% bovine serum albumin (BSA), pH 7.4 (with KOH). Substrates were either 5 mM succinate plus 1µM rotenone plus 2mM phosphate, 5mM glycerol-3-phosphate plus 1µM rotenone or 5mM pyruvate plus 3mM malate. GDP (1mM final) was added when indicated. Fluorescence was detected by Perkin Elmer LS 55 Fluorometer with excitation set at 570±8nm and emission at 585±4nm. The temperature throughout the experiment was maintained at 28°C. Superoxide

release from brown adipose tissue mitochondria, measured using dihydroethidium (DHE)(Molecular Probes), was performed exactly as described by Shabalina et al. [28] and measurements were made within the same time frame as these authors. Mitochondria (0.5mg) were respiring on 5mM glycerol-3-phosphate in the presence of 1 $\mu$ g/ml rotenone, DHE (50 $\mu$ M) and antimycin A (1.2 $\mu$ g/ml). The fluorescence emitted by ethidium was followed on the Perkin Elmer LS 55 Fluorometer at 37°C with excitation set at 495nm and emission at 580nm.

#### *2.4 Detection of the mitochondrial electrochemical gradient across the inner membrane ( $\Delta \Psi_m$ ).*

Membrane potential of isolated mitochondria was examined by fluorescent dye safranin, which accumulates and quenches in polarized mitochondria [32]. Assay medium consisted of mitochondria (0,125 mg/ml), 5 $\mu$ M safranin, 60 mM sucrose, 30 mM KCl, 20 mM Tris, 1 mM EDTA, 1 mM EGTA, 0.1 % BSA, pH 7.4 (KOH). Substrates were either 5 mM succinate plus 1 $\mu$ M rotenone plus 2mM phosphate, 5mM glycerol-3-phosphate plus 1 $\mu$ M rotenone or 5mM pyruvate plus 3mM malate. 1mM GDP, 0.5 $\mu$ M protonophore carbonyl-4-(trifluoromethoxy)-phenylhydrazone (FCCP) were added where indicated. Fluorescence was detected by Perkin Elmer LS 55 Fluorometer with excitation set at 523 $\pm$ 3 nm and emission at 580 $\pm$ 6.7 nm and the temperature of medium was maintained at 28°C.

### *2.5 Measurement of Oxygen consumption rates of mitochondria*

All measurements of respiration were made using an Oxygraph-2k respirometer (Oroboros Instruments, Innsbrück, Austria), and oxygen flux was resolved using DATLAB software. The oxygraph-2k is a two chamber titration-injection respirometer with a limit of oxygen flux detection of  $1\text{pmol s}^{-1}\text{ml}^{-1}$ . Standardized instrumental and chemical calibrations were performed to correct for back diffusion of oxygen into the chamber from the various components; leak from the exterior, oxygen consumption by the chemical medium, and sensor oxygen consumption. The mitochondrial suspension was stirred using a polyvinylidene difluoride (PVDF) magnetic stirrer and thermostatically maintained at  $28^{\circ}\text{C}$ . BAT mitochondria were incubated in 60mM sucrose, 30mM KCl, 20mM Trizma-base, 1mM EDTA, 1mM EGTA, 1 $\mu\text{M}$  atractyloside, 1 $\mu\text{g/ml}$  oligomycin and 0.1% de-fatted BSA, pH 7.4. Before each experiment the medium was equilibrated for 30-40 minutes with air in the oxygraph chambers until a stable signal was achieved to calibrate for oxygen saturation. Steady state oxygen consumption rates (state 4) were then measured in the presence of the substrate of interest. Substrates were either 5 mM succinate plus 1 $\mu\text{M}$  rotenone plus 2mM phosphate, 5mM glycerol-3-phosphate plus 1 $\mu\text{M}$  rotenone or 5mM pyruvate plus 3mM malate. Subsequent additions of 1mM GDP and 0.5 $\mu\text{M}$  protonophore carbonyl-4-(trifluoromethoxy)-phenylhydrazine (FCCP) were added.

## 2.6 Statistics

All data are expressed as means  $\pm$  S.E.M. of at least 3 separate experiments performed in triplicate. Statistical differences were determined by a two-tail unpaired student's t-test. Unless otherwise stated a p value of  $\leq 0.05$  was taken to indicate significance.

## 3. Results

In Figure 1 we see examples of primary data showing time courses of the production of Amplex Red fluorescence in the medium, as a result of non-phosphorylating isolated brown adipose tissue mitochondria respiring on a variety of substrates. The increased fluorescence by Amplex Red indicates an increased rate of  $H_2O_2$  production which in turn indicates an increased rate of ROS production by mitochondria. It was observed that in all instances, there is a continuous increase in Amplex Red fluorescence, over time, for all electron transport chain substrates used (succinate, glycerol-3-phosphate or pyruvate/malate) (A-F). In addition, GDP, an inhibitory ligand for UCP 1, increases the rate of  $H_2O_2$  production in mitochondria from wild-type mice (A-C) whereas ROS production by mitochondria from UCP 1 knock-out mice appears equivalent to that by mitochondria from wild-type mice in the presence of GDP. Reassuringly, GDP has no effect on ROS production by mitochondria from UCP 1 knock-out mice (D-F). It should be noted that we

also looked at detection of reactive oxygen species in isolated BAT mitochondria from wild-type and UCP 1 knock-out mice using dichlorodihydrofluorescein diacetate (DCFDA) and observed a difference in the rate of reactive oxygen species production (results not shown) similar in magnitude to that observed for Amplex Red. However, we chose the Amplex RED detection system as we were able to obtain consistently linear rates of changes in fluorescence.

Primary data for the detection of H<sub>2</sub>O<sub>2</sub> generation by isolated brown adipose tissue mitochondria were collated and are presented in Figure 2. The graphs show data for mitochondria respiring under non-phosphorylating conditions from wild-type and UCP1 knock-out mice for electron transport chain substrates (succinate, glycerol-3-phosphate or pyruvate/malate) in the presence and absence of GDP. The data demonstrate a significant difference in generation of H<sub>2</sub>O<sub>2</sub> on addition of GDP to mitochondria from wild-type mice for all substrates investigated; succinate plus rotenone (0.12±0.015 to 0.17±0.001, p, 0.035), glycerol-3-phosphate (0.46±0.06 to 0.86±0.12. p, 0.022), pyruvate plus malate (0.046±0.012 to 0.110±0.028, p, 0.05). In addition, the data demonstrate a significant difference in the rate of generation of H<sub>2</sub>O<sub>2</sub> in a comparison of isolated brown adipose tissue mitochondria from wild-type mice without GDP versus UCP 1 knock-out mice without GDP: succinate plus rotenone (0.12±0.015 to 0.18±0.015, p, 0.033), glycerol-3-phosphate (0.46±0.06

to  $0.92 \pm 0.15$ ,  $p$ , 0.030), pyruvate plus malate ( $0.046 \pm 0.012$  to  $0.11 \pm 0.03$ ,  $p$ , 0.044). There was no significant difference in generation of  $H_2O_2$  in a comparison of isolated brown adipose tissue mitochondria from wild-type mice with GDP compared to mitochondria from UCP 1 knock-out mice with or without GDP: succinate plus rotenone ( $0.18 \pm 0.015$  versus  $0.185 \pm 0.015$ ); glycerol-3-phosphate ( $0.92 \pm 0.15$  versus  $1.00 \pm 0.09$ ); pyruvate plus malate ( $0.085 \pm 0.004$  versus  $0.086 \pm 0.004$ ). A further point to note is that the rate of production of reactive oxygen species by isolated brown adipose tissue mitochondria, in the presence or absence of GDP for wild-type mice and in the presence or absence of GDP for UCP 1 knock-out mice, is greater for different substrates according to the following order: glycerol-3-phosphate > succinate > pyruvate plus malate. Similar results to those for brown adipose tissue mitochondria from wild-type mice were observed for mitochondria from rat brown adipose tissue in all instances (results not shown).

Figure 3A shows that no difference in superoxide production rates are evident when dihydroethidium (DHE) is added to measure the rate of superoxide production in a comparison of mitochondria from wild-type and UCP 1 knock-out mice. In this instance 5mM glycerol-3-phosphate was used as substrate in the presence of 2 $\mu$ g/ml rotenone. Furthermore, there is an equivalent modest increase in the rate of ethidium fluorescence on addition of antimycin to mitochondria from wild-type and UCP 1 knock-out mice. In Figure 3B we see that the rate of ROS production, as detected by Amplex Red,

is greater in mitochondria from UCP 1 knock-out mice compared to those from wild-type mice. Furthermore, addition of antimycin increases the rate of ROS production from both sources of mitochondria, as expected, but the rate is dramatically greater in mitochondria from wild-type mice. As expected, the uncoupler FCCP decreases ROS production detected by Amplex Red in mitochondria from both wild-type and UCP 1 knock-out mice (Figure 3C).

Figure 4 has representative primary data depicting the profile of safranin fluorescence in non-phosphorylating brown adipose tissue mitochondria from wild-type and UCP 1 knock-out mice, for a variety of electron transport chain substrates, and in the presence and absence of GDP. The measured fluorescence is due to safranin in the medium. Mitochondria with a high membrane potential will accumulate safranin from the medium, thus registering a decrease in safranin fluorescence. In figure 4A, we see a modest drop in medium fluorescence (~25 units) on addition of electron transport chain substrates to mitochondria isolated from brown adipose tissue of wild-type animals. The drop in fluorescence is augmented (~500 units) on addition of GDP for all substrates (succinate plus rotenone, glycerol-3-phosphate, pyruvate plus malate) (Fig. 4A). As expected, on addition of the uncoupler, FCCP, the safranin is released from the mitochondria back into the medium and fluorescence increases for all substrates (Fig. 4A). In contrast to mitochondria from wild-type mice, we see a large drop (~500 units) in medium fluorescence on addition of electron transport chain substrates

(succinate plus rotenone, glycerol-3-phosphate, pyruvate plus malate) to mitochondria from UCP1 knock-out mice (Fig. 4B). Furthermore and in contrast to mitochondria from wild-type mice, GDP has no effect on fluorescence no matter what the substrate (Fig. 4B). As expected and like mitochondria from wild-type mice, the safranin is released from the mitochondria back into the medium and fluorescence increases, for all substrates on addition of uncoupler to mitochondria from UCP 1 knock-out mice (Fig. 4B). Similar results to those for brown adipose tissue mitochondria from wild-type mice were observed for mitochondria from rat brown adipose in all instances (results not shown).

Figure 5 shows data for oxygen consumption rates measured for isolated brown adipose tissue mitochondria from wild-type and UCP 1 knock-out mice. Mitochondria were incubated under non-phosphorylating conditions with succinate, glycerol-3-phosphate or pyruvate plus malate in the presence and absence of GDP. The data in Figure 5A demonstrate a significant decrease in oxygen consumption rate on addition of GDP to mitochondria from wild-type mice respiring on succinate plus rotenone ( $103 \pm 10$  to  $50 \pm 3$ ,  $p$ , 0.0118) and in a comparison of mitochondria from wild-type and UCP 1 knock-out mice ( $103 \pm 10$  to  $60 \pm 3$ ,  $p$ , 0.04). The data in Figure 5B demonstrate a significant decrease in oxygen consumption rates on addition of GDP to mitochondria from wild-type mice respiring on glycerol-3-phosphate ( $139 \pm 12$  to  $75 \pm 4$ ,  $p$ , 0.0177) and in a comparison of mitochondria from wild-type and UCP 1

knock-out mice using glycerol-3-phosphate ( $139\pm 12$  to  $100\pm 5$ ,  $p$ , 0.0459). The data in Figure 5C demonstrate a significant decrease in oxygen consumption rates on addition of GDP to mitochondria from wild-type mice respiring on pyruvate plus malate ( $51\pm 12$  to  $15\pm 1$ ,  $p$ , 0.0433) and in a comparison of mitochondria from wild-type and UCP 1 knock-out mice using pyruvate plus malate ( $51\pm 12$  to  $15\pm 2$ ,  $p$ , 0.0396). GDP had no significant effect on oxygen consumption by mitochondria for UCP1 knock-out mice for succinate plus rotenone ( $60\pm 10$  versus  $52\pm 10$ ), glycerol-3-phosphate plus rotenone ( $100\pm 5$  to  $105\pm 10$ ) and pyruvate plus malate ( $15\pm 2$  versus  $15\pm 1$ ). The addition of the uncoupler, FCCP, after GDP addition, increased oxygen consumption by mitochondria in all instances. Similar results to those for brown adipose tissue mitochondria from wild-type mice were observed for mitochondria from rat brown adipose tissue in all instances (results not shown).

#### 4. Discussion

In this study we investigated whether there was a role for UCP 1 in the generation of reactive oxygen species (ROS) by mitochondria from brown adipose tissue by comparing mitochondria from wild-type and UCP 1 knock-out mice. In Figures 1 and 2 we have provided evidence that ablation of UCP 1 increases the rate of ROS production by mitochondria from brown adipose tissue when compared to mitochondria from wild-type controls, no matter

what electron transport chain substrate is used. These observations of increased ROS production by mitochondria from UCP 1 knock-out mice are mirrored by the addition of the purine nucleotide, GDP, a known inhibitor of UCP 1 function, to brown adipose tissue mitochondria from wild-type animals. Reassuringly and as expected, GDP has no effect on ROS production by UCP 1 knock-out mice.

Our experiments with UCP1 knock-out mice provide the proof that activity of UCP 1, not UCP 2 or UCP3, regulates ROS production in brown adipocyte tissue mitochondria. We know of one other study investigating the role of UCP 1 in ROS production for isolated mitochondria from brown adipose tissue of mice. In that study, there was no difference in the rate of production of ethidium fluorescence, before and after addition of antimycin, in a comparison of mitochondria from wild-type and UCP 1 knock-out mice respiring on glycerol-3-phosphate [28], an observation we can confirm as we make the same observation under the exact same experimental conditions as those authors (Figure 3A). By contrast, in Figure 3B the difference in ROS production rate, in a comparison of mitochondria from wild-type and UCP 1 knock-out mice, is immediately evident on addition Amplex Red, with the subsequent addition of antimycin increasing ROS production rate in both sources of mitochondria and dramatically in mitochondria from wild-type mice. The expected decrease in ROS production on addition of FCCP, as detected by Amplex Red is evident in Figure 3C.

The data in Figure 3, in particular the comparison of data from mitochondria of wild-type mice presented in Figure 3A and 3B before and after antimycin addition, illustrates that Amplex Red detection of  $H_2O_2$  is a much more sensitive assay of actual reactive oxygen species production than detection of superoxide directly and alone by DHE. It should also be pointed out that the data we present in Figure 1 and 2, using Amplex Red, for mice (respiring on succinate plus rotenone, glycerol-3-phosphate and pyruvate plus malate), are internally consistent with expected differences in ROS production, in that ROS production by brown adipose tissue mitochondria from UCP1-knockout mice is greater than that for mitochondria from wild-type mice, yet the same as that for wild-type mice plus GDP and consistent with our data for rats (not shown) where ROS production (detected using Amplex Red), was increased on addition of GDP to mitochondria (respiring on succinate plus rotenone, glycerol-3-phosphate and pyruvate plus malate) from brown adipose tissue. Our data for wild-type mice are also consistent with data for rats from other laboratories where ROS production was increased on addition of GDP to mitochondria from brown adipose tissue respiring on succinate [33] and pyruvate plus malate [32].

The effect of UCP 1 ablation or UCP 1 inhibition on ROS production is reassuringly mirrored by our observations that mitochondrial membrane potential is maximal when UCP 1 is inhibited (Fig. 4A) or ablated (Fig. 4B). The high membrane potential and subsequent increased production of ROS is

consistent with more reduced redox couples in the electron transport chain, particularly the ubiquinone/ubisemiquinone redox couple in the P-site of complex III [6,16].

The oxygen consumption rates for mitochondria of brown adipose tissue were also measured in parallel to ROS production and membrane potential. The data show that mitochondria from UCP 1 ablated mice or from wild-type mice where UCP 1 has been inhibited have decreased oxygen consumption rates, when comparing mitochondria from wild-type mice in the absence of GDP, respiring on succinate in the presence of rotenone (Fig. 5A), glycerol-3-phosphate in the presence of rotenone (Fig. 5B) and pyruvate plus malate (Fig. 5E). These data are consistent with high membrane potential and consequent increased production of ROS due to a more reduced ubiquinone/ubisemiquinone redox couple in the P-site of complex III [6,16]. It should be noted that although it was necessary to measure membrane potential and oxygen consumption in brown adipose tissue mitochondria from wild-type and UCP 1 knock-out mice as part of the controls for this study (figures 4 and 5), these parameters have been measured under similar conditions by others [34-36] and our data are consistent with the data in these studies.

The data in Figures 1 and 2 also demonstrate that ROS production by brown adipose tissue mitochondria from wild-type or UCP 1 knock-out animals, in

the presence or the absence of GDP, was greater when glycerol-3-phosphate was used as substrate, than when succinate (plus rotenone) or pyruvate plus malate were used.

This observation is consistent with the observations of Drahota et al. [8] and Vrbacký et al [11] who showed that ROS production by mitochondria isolated from brown adipose tissue of the Syrian hamster is greater for glycerol-3-phosphate when compared with that for succinate (plus rotenone). It should also be noted that BAT mitochondria and indeed mitochondria from UCP1-knock-out mice contain UCP 2 and UCP 3 [29, 35], proteins which are apparently not compensating for UCP 1 in the UCP1 ablated mice.

Hence, with the potential for increased ROS production in BAT of UCP 1 knock-out mice, one might expect increased anti-oxidant capacity in the BAT of these mice. A comparison of the anti-oxidant defence systems of wild-type and UCP1 knock-out mice has been reported [28], however no increase in (a) MnSOD, (b) CuZnSOD, (c) catalase or (d) ROS sensitive aconitase activity in brown adipose tissue mitochondria from UCP1 knock-out mice compared to mitochondria from wild-type mice.

In summary, we conclude that UCP 1 in brown adipose tissue mitochondria plays a role in regulating ROS production by isolated mitochondria and thus may play a similar role in situ.

## Acknowledgements

This work was supported by grants from Marie Curie Transfer of Knowledge grant COMPIB MTKD-CT-2005-030005 and Science Foundation Ireland Principal Investigator Grant SFI 06/IN.1/B67. Andrea Dlasková was on an extended leave of absence from the Institute of Physiology, Academy of Sciences of the Czech Republic.

## References

- [1] Chance, B., Sies, H. and Boveris, A. (1979) Hydroperoxide metabolism in mammalian organs. *Physiol. Rev.* 59, 527-605.
- [2] Turrens, J.F. (2003) Mitochondrial formation of reaction oxygen species. *J. Physiol.* 552, 335-344.
- [3] Grivennikova, V.G. and Vinogradov, A.D. (2006) Generation of superoxide by the mitochondrial complex I. *Biochim. Biophys. Acta* 1757, 553-561.
- [4] Boveris, A., Valdez, L.B., Zaobornyj, T. and Bustamante, J. (2006) Mitochondrial metabolic states regulate nitric oxide and hydrogen peroxide diffusion to the cytosol. *Biochim. Biophys. Acta* 1757, 535-542.
- [5] Lambert A.J. and Brand, M.D. (2004) Superoxide production by NADH:ubiquinone oxidoreductase (complex I) depends on the pH

- gradient across the mitochondrial inner membrane. *Biochem. J.* 382, 511-517.
- [6] Andreyev, A.Y., Kushnareva, Y.E. and Starkov, A.A. (2005) Mitochondrial metabolism of reactive oxygen species. *Biochemistry (Moscow)* 70, 246-264.
- [7] Miwa, S., St-Pierre, J., Patridge, L. and Brand, M.D. (2003) Superoxide and hydrogen peroxide production by *Drosophila* mitochondria, *Free Radic. Biol. Med.* 35, 938-948.
- [8] Drahotá, Z., Chowdhury, S.K., Floryk, D., Mráček, T., Wihelm, J., Rauchová, H., Lenaz, G. and Houštěk, J. (2002) Glycerophosphate-dependent hydrogen peroxide production by brown adipose tissue mitochondria and its activation by ferricyanide. *J. Bioenerg. Biomembr.* 34, 105-113.
- [9] Genova, M.L., Pich, M.M., Biondi, A., Bernacchia, A., Falasca, A., Bovina, C., Formiggini, G., Castelli, G.P. and Lenaz, G. (2003) Mitochondrial production of oxygen radical species and the role of coenzyme Q as an antioxidant. *Exp. Biol. Med.* 228, 506-513.
- [10] Muller, F.L., Liu, Y. and Van Remmen, H. (2004) Complex III releases superoxide to both sides of the inner mitochondrial membrane. *J. Biol. Chem.* 279, 49064-49073.
- [11] Vrbacký, M., Drahotá, Z., Mráček, T., Vojtíšková, A., Ješina, P., Stopka, P. and Houštěk, J. (2007) Respiratory chain components involved in

glycerolphosphate dehydrogenase-dependent ROS production by brown adipose mitochondria. *Biochim. Biophys. Acta* 1767, 989-997.

- [12] Nomura, K., Imai, H., Koumura, T., Kobayashi, T and Nakagawa, Y. (2000) Mitochondrial phospholipid hydroperoxide glutathione peroxidase inhibits the release of cytochrome c from mitochondria by suppressing the peroxidation of cardiolipin in hypoglycaemia induced apoptosis. *Biochem. J.* 351, 183-193.
- [13] Paradies, G., Petrosillo, G., Pistolese, M. and Ruggiera, F.M. (2000) The effect of reactive oxygen species generated from the mitochondrial electron transport chain on the cytochrome c oxidase activity and on the cardiolipin content of bovine heart submitochondrial particles. *FEBS Lett.* 466, 323-326.
- [14] Ernster, L. (1993) Lipid peroxidation in biological membranes: mechanism and implications. In: *Active oxygen, lipid peroxides, and antioxidants* (K. Yagi, ed.), Japan Science Society Press, Tokyo, pp1-38.
- [15] Sayre, L.M., Lin, D., Yuan, Q., Zhu, X. and Tang, X. (2006) Protein adducts generated from products of lipid oxidation: focus on HNE and ONE. *Drug Metab. Rev.* 38, 651-675.
- [16] Ježek, P. and Hlvatá, L. (2005) Mitochondria in homeostasis of reactive oxygen species in cell, tissues, and organism. *Int. J. Biochem. Cell Biol.* 37, 2478-2503.

- [17] Forsmark-Andrée, P., Dallner, G. and Ernster, L. (1995) Endogenous ubiquinol prevents protein modification accompanying lipid peroxidation in beef heart submitochondrial particles. *Free Radic. Biol. Med.* 19, 749-757.
- [18] Ham, A.J. and Lieber, D.C. (1995) Vitamin E oxidation in rat liver mitochondria. *Biochemistry* 34, 5754-5761.
- [19] Fridovich, I. (1998) Oxygen toxicity: A radical explanation, *J. Exp. Biol.* 201, 1203-1209.
- [20] Skulachev, V.P. (1996) Role of uncoupled and non-coupled oxidations in maintenance of safely low levels of oxygen and its one-electron REDuctants. *Q. Rev. Biophys.* 29, 169-202.
- [21] Brand, M.D., Affourtit, C., Esteves, T.C., Green, K., Lambert, A.J., Miwa, S., Pakay, J.L. and Parker, N. (2004) Mitochondrial superoxide: production, biological effects, and activation of uncoupling proteins. *Free Radic. Biol. Med.* 37, 755-767.
- [22] Talbot, D.A. and Brand, M.D. (2005) Uncoupling protein 3 protects aconitase against inactivation in isolated skeletal muscle mitochondria. *Biochim. Biophys. Acta* 1709, 150-156.
- [23] McLeod, C.J., Abdulhameed, A., Hoyt, R.F., McCoy, J.P. and Sack, M.N. (2005) Uncoupling proteins 2 and 3 function in concert to augment tolerance to cardiac ischaemia. *J. Biol. Chem.* 280, 33470-33476.

- [24] Bai, Y., Onuma, H., Bai, X., Madvedev, A.V., Misukonis, M., Weinberg, J.B., Cao, W., Robidoux, J., Floering, L.M., Daniel, K.W. and Collins, S. (2005) Persistent nuclear factor- $\kappa$ B activation in UCP2<sup>-/-</sup> mice leads to enhanced nitric oxide and inflammatory cytokine production. *J. Biol. Chem* 19, 19062-19069.
- [25] Arsenijevic, D., Onuma, H., Pecqueur, C., Raimbault, S., Manning, B.S., Miroux, B., Couplan, E., Alves-Guerra, M-C., Goubert, M., Surwit, R., Bouillaud, F., Richard, D., Collins, S., and Ricquier, D. (2000) Disruption of the uncoupling protein-2 gene in mice reveals a role in immunity and reactive oxygen species production, *Nature Genetics* 26, 435-439.
- [26] Echtay, K.S., Roussel, D., St-Pierre, J., Jekabsons, M.B., Cadenas, S., Stuart, J.A., Harper, J.A., Roeback, S.J., Morrison, A., Pickering, S., Clapham, J.C. and Brand, M.D. (2002) Superoxide activates mitochondrial uncoupling proteins. *Nature* 415, 96-99.
- [27] Echtay, K.S., Esteves, T.C., Pakay, J.L., Jekabsons, M.B., Lambert, A.J., Portero-Otín, M., Pamplona, R., Vidal-Puig, A.J., Wang, S., Roeback, S.J. and Brand, M.D. (2003) A signalling role for 4-hydroxy-2-nonenal in regulation of mitochondrial uncoupling. *The EMBO Journal* 22, 4103–4110.
- [28] Shabalina, I.G., Petrovic, N., Kramarova, T.V., Hoeks, J, Cannon, B. And Nedergaard, J. (2006) UCP1 and defense against oxidative stress: 4-hydroxy-nonenal effects on brown adipose-fat mitochondria are uncoupling 1 independent. *J. Biol. Chem.* 281, 13882-13893.

- [29] Nedergaard, J., Golozoubova, V., Matthias, A., Abolfazl, A., Jacobsson, A. and Cannon, B. (2001) UCP1: the only protein able to mediate adaptive non-shivering thermogenesis and metabolic inefficiency, *Biochim. Biophys. Acta* 1505, 82-106.
- [30] Scarpace, P.J., Bender, B.S. and Borst, S.E. (1991) *Escherichia coli* peritonitis activates thermogenesis in brown adipose tissue: relationship to fever. *Can. J. Physiol. Pharmacol.* 69, 761-767.
- [31] Smith, P.K., Krohn, R.I., Hermanson, G.T., Mallia, A.K., Gartner, F.H., Provenzano, M.D., Fujimoto, E.K., Goeke, N.M., Olson, B.J. and Klenk, D.C. (1985) Measurement of protein using bicinchoninic acid. *Anal. Biochem.* 150, 76-85.
- [32] Dlasková, A., Špaček, T., Škobisová, E., Šantorová, J. and Ježek, P. (2006) Certain aspects of uncoupling due to mitochondrial uncoupling proteins in vitro and in vivo. *Biochim. Biophys. Acta* 1757, 467-473.
- [33] Nègre-Salvayre, A., Hirtz, C., Carrera, G., Cazenave, R., Trolly, M., Salvayre, R., Pénicaud, L. Casteilla, L. (1997) A role for uncoupling protein-2 as a regulator of mitochondrial hydrogen peroxide generation. *FASEB J.* 11, 809-815.
- [34] Monemdjou, S., Kozak, L.P. and Harper, M-E. (1999) Mitochondrial proton leak in brown adipose tissue mitochondria of UCP1-deficient mice is GDP insensitive. *Am. J. Physiol. Endocrinol. Metab.* 276, E1073-E1082.

- [35] Matthias, A., Jacobsson, A., Cannon, B. and Nedergaard, J. (1999) the Bioenergetics of brown fat mitochondria from UCP-1 ablated mice. *J. Biol. Chem.* 274, 28150-28160.
- [36] Shabalina, I.G., Jacobsson, A., Cannon, B. and Nedergaard, J. Native UCP 1 displays simple competitive kinetics between the regulators purine nucleotides and fatty acids. (2004) *J. Biol. Chem.* 274,

## FIGURE LEGENDS

Figure 1.

Examples of time courses for the detection of H<sub>2</sub>O<sub>2</sub> generation in isolated brown adipose tissue mitochondria using Amplex Red.

The graphs show examples of the primary time course data for generation of H<sub>2</sub>O<sub>2</sub> in isolated brown adipose tissue mitochondria using Amplex Red from wild-type (A-C) and UCP 1 knock-out mice (D-F) in the presence and absence of GDP (1mM). Mitochondria were incubated under non-phosphorylating conditions as described in the methods section. The electron transport chain substrates used were: (A & D) 5 mM succinate plus 1 μM rotenone, (B & E) 5 mM glycerol-3-phosphate plus 1 μM rotenone; (C & F) 5mM pyruvate plus 3mM malate. Data represent typical traces of individual readouts.

Figure 2.

Collated data for the detection of H<sub>2</sub>O<sub>2</sub> generation in isolated brown adipose tissue mitochondria

The graphs show collated data for generation of H<sub>2</sub>O<sub>2</sub> in isolated brown adipose tissue mitochondria from wild-type and UCP 1 knock-out mice plus or minus GDP (1mM). Mitochondria were incubated under non-phosphorylating conditions as described in the methods section. The electron transport chain substrates used are 5 mM succinate plus 1  $\mu$ M rotenone, 5 mM glycerol-3-phosphate plus 1  $\mu$ M rotenone and 5 mM pyruvate plus 3 mM malate. Data represent mean  $\pm$ sem of at least three separate experiments performed in at least triplicate. 'p' values were determined using an unpaired students 't' test. In a comparison of mitochondria from wild-type mice in the presence and absence of GDP, the following values were calculated: succinate plus rotenone (p, 0.035), glycerol-3-phosphate (p, 0.022), pyruvate plus malate (p, 0.05). In a comparison of mitochondria from wild-type mice without GDP versus UCP 1 knock-out mice without GDP, the following values were calculated: succinate plus rotenone (p, 0.033), glycerol-3-phosphate (p, 0.030), pyruvate plus malate (p, 0.044).

Figure 3. Primary data showing time courses for the detection of ethidium and Amplex Red fluorescence in brown adipose tissue mitochondria from wild-type and UCP 1 knock-out mice.

(A) Superoxide release measured using dihydroethidium (DHE)(Molecular Probes) was determined as described by Shabalina et al. [28]. Mitochondria (0.5mg) were respiring on 5mM glycerol-3-phosphate in the presence of 1 $\mu$ g/ml rotenone. DHE (50 $\mu$ M) and antimycin A (1.2 $\mu$ g/ml) were added where indicated. (B) Mitochondria (0.125mg/ml) were respiring on 5mM glycerol-3-phosphate in the presence of rotenone (1 $\mu$ M). Amplex Red (5 $\mu$ M) and antimycin A (1.2 $\mu$ g/ml) were added where indicated. (C) Mitochondria (0.125mg/ml) were respiring on 5mM succinate in the presence Amplex Red (5 $\mu$ M) and rotenone (1 $\mu$ M). GDP (1mM) and FCCP (0.5 $\mu$ M) were added where indicated.

Figure 4.

Profile of mitochondrial membrane potential in isolated brown adipose tissue mitochondria.

The data represent the use of safranin fluorescence to generate primary data indicating a qualitative measure of membrane potential, across the inner membrane of mitochondria isolated from brown adipose tissue of (A) wild-type and (B) UCP 1 knock-out mice. Mitochondria are incubated under non-phosphorylating conditions as described in the methods section. The electron

transport chain substrates used were: (a) 5 mM succinate plus 1  $\mu$ M rotenone; (b) 5 mM glycerol-3-phosphate plus 1  $\mu$ M rotenone; (c) 5 mM pyruvate plus 3 mM malate. GDP (1 mM) was added approximately 400s after addition of substrate and the uncoupler FCCP was added approximately 400s after addition of GDP. Data represent typical traces of individual readouts.

Figure 5.

Non-phosphorylating oxygen consumption by isolated brown adipose tissue mitochondria

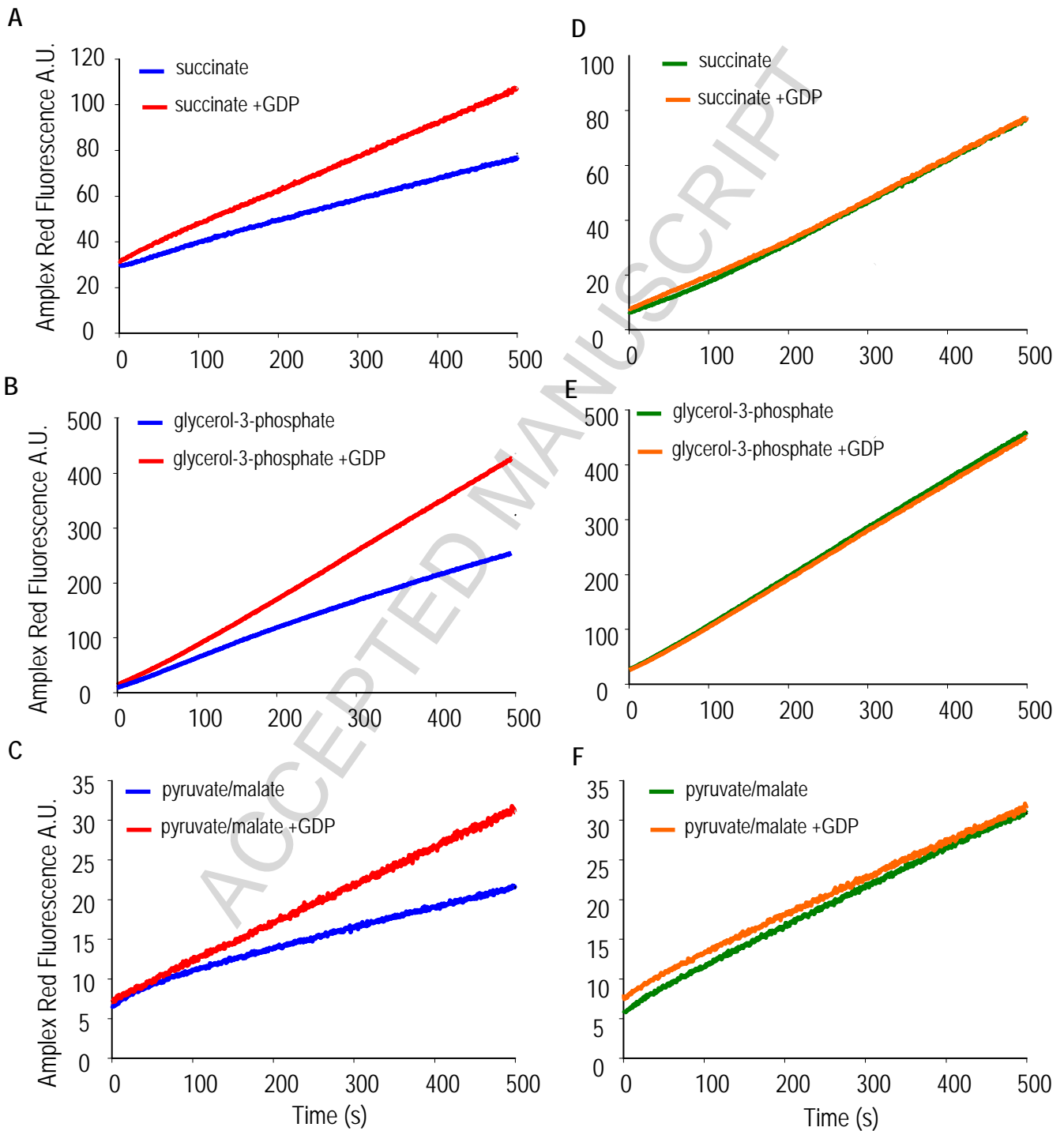
The graphs show collated data for oxygen consumption rates measured for isolated brown adipose tissue mitochondria from wild-type and UCP 1 knock-out mice. Mitochondria were incubated under non-phosphorylating conditions as described in the methods section. The electron transport chain substrates used are (A) 5 mM succinate plus 1  $\mu$ M rotenone, (B) 5 mM glycerol-3-phosphate plus 1  $\mu$ M rotenone and (C) 5 mM pyruvate plus 3 mM malate. GDP (1mM) was added approximately 400s after addition of substrate and the uncoupler FCCP was added approximately 400s after addition of GDP. Data represent mean  $\pm$  sem of at least three separate experiments

performed in at least triplicate 'p' values were determined using an unpaired students 't' test. In a comparison of mitochondria from wild-type mice in the presence and absence of GDP, the following values were calculated: succinate plus rotenone (p, 0.0118), glycerol-3-phosphate (p, 0.0177), pyruvate plus malate (p, 0.0433). In a comparison of mitochondria from wild-type mice without GDP versus UCP 1 knock-out mice without GDP, the following values were calculated: succinate plus rotenone (p, 0.04), glycerol-3-phosphate (p, 0.0459), pyruvate plus malate (p, 0.0396).

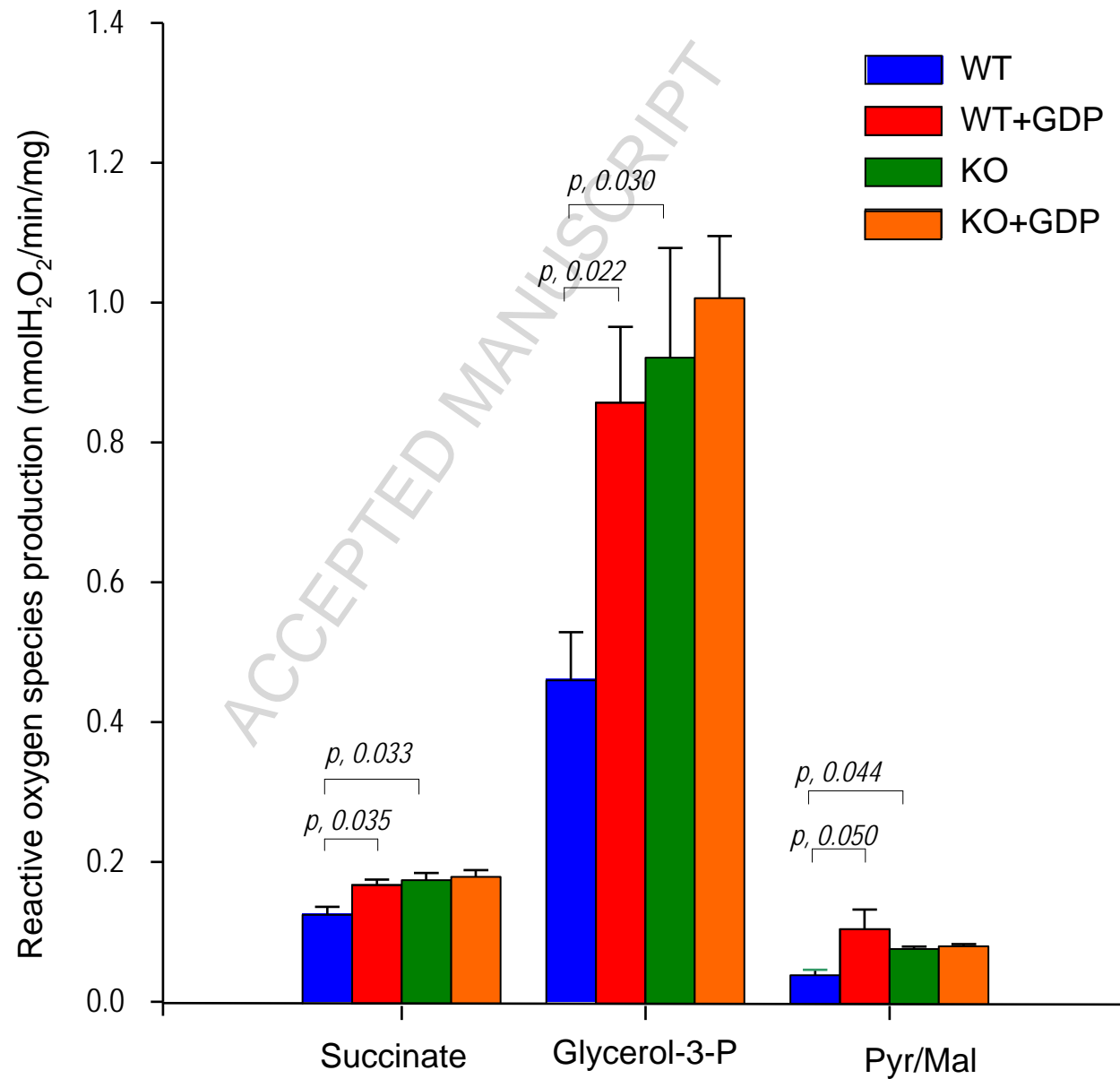
Dlasková et al. Figure 1

Wild-type

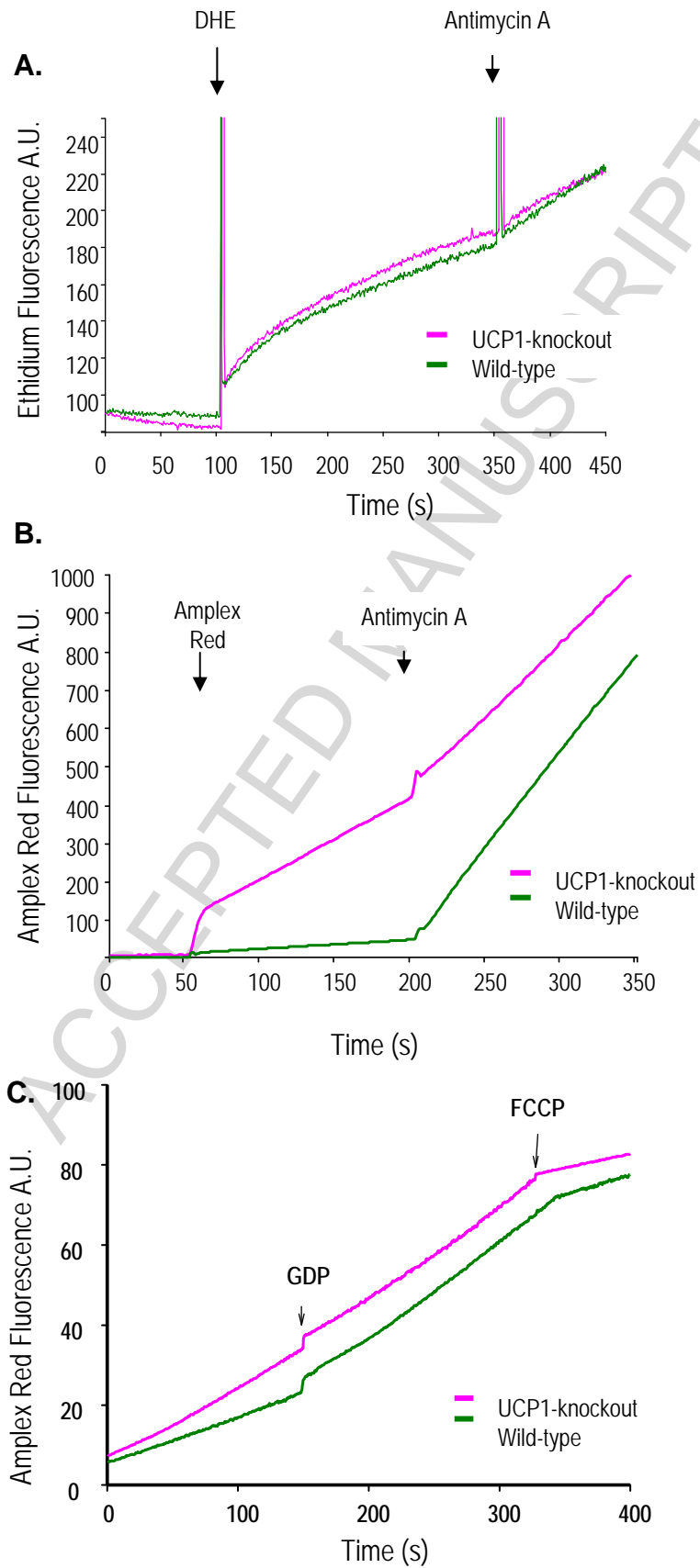
UCP1-knockout



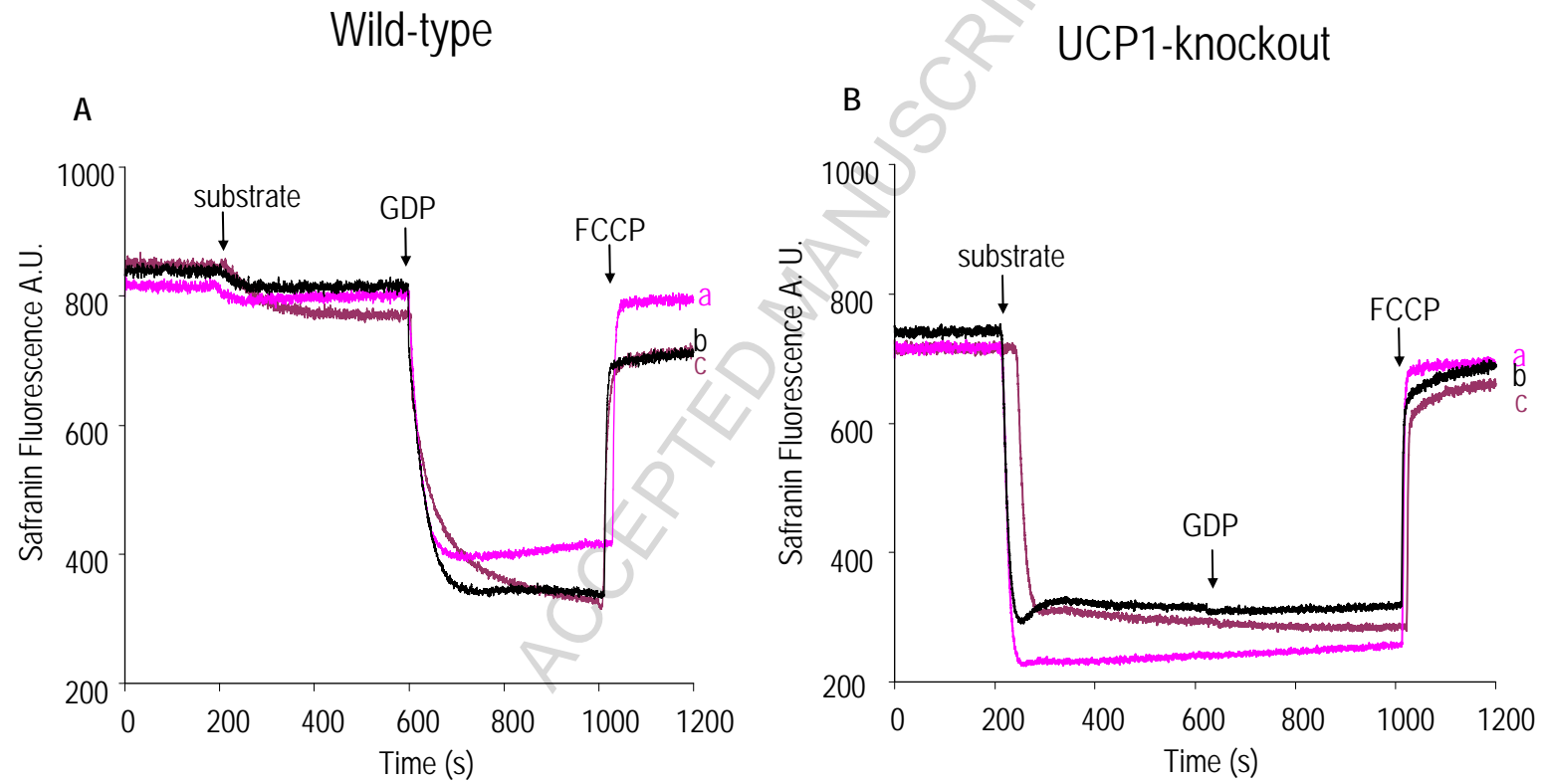
Dlasková et al. Figure 2



Dlasková et al. Figure 3



Dlasková et al. Figure 4



Dlasková et al. Figure 5

